Satellite coverage assessment considering cloud cover

Ciara N. McGrath*
University of Manchester, Oxford Road, M13 9PL, Manchester, England, United Kingdom.

Astrid Werkmeister †, Joshua Gribben ‡, Christopher J. Lowe §, and Malcolm Macdonald ¶
Applied Space Technology Laboratory, Department of Electronic & Electrical Engineering, University of Strathclyde, 204 George St, Glasgow, G1 1XW, United Kingdom.

Due to cloud cover, the performance provided by optical or lidar satellite systems may differ from the predicted performance. This work presents a means of rapidly assessing the coverage that can be expected from a satellite constellation considering cloud probability. A latitude-specific pseudo-circumference is defined and calculated using a cloud factor to provide insights into the relative coverage available to different regions. Comparison of the results from the presented method with simulated and historical data collected by the Sentinel-2 constellation shows the potential of the proposed method to calculate expected time between cloud free images when averaged over the long-term. Appropriate choice of cloud model is found to be an important consideration to ensure the validity of the method.

I. Introduction

The challenge of designing satellite constellations to provide global, regional, and zonal coverage of the Earth has been studied in detail [1–10]. However, for many systems, such as optical, lidar, or laser-to-ground communications, the impact of cloud may mean that the system performance in reality differs significantly from the ideal [11–13]. This can have a measurable impact on mission outcomes as, for example, demonstrated by [14], which found that greater deforestation occurred in Brazilian rainforests during periods when the view from their satellite detection and alert system was obscured by cloud. Accounting for the impact of cloud cover at the design phase could, therefore, improve operational performance by planning systems from the outset to focus coverage on hard-to-observe regions and give an improved probability of meeting the desired performance.

This work proposes a method of rapidly assessing the expected coverage of a region by a satellite, or constellation of satellites, considering the impact of cloud cover. This fast approach, while inexact, is valuable as the trend for higher resolution satellite data (0.3m - 5m), with correspondingly smaller fields of view, continues. Traditional coverage analysis relies on numerical propagation of orbits and assessment via a computationally intensive grid point approach;

*Lecturer in Aerospace Systems, AIAA Young Professional Member.
†Knowledge Exchange Associate.
‡PhD Student.
§Research Fellow.
¶Professor and Chair of Applied Space Technology, AIAA Associate Fellow.

alternative methods have been proposed but they still become time consuming, and even intractable, for constellations with many spacecraft [15]. The coverage calculation approach selected for this work uses an analytical method of coverage estimation, but this is decoupled from the consideration of cloud cover such that it could be replaced by an alternative higher fidelity method of coverage calculation as desired.

II. Method

A. Assumptions

The method of coverage estimation used and described herein is valid for the following assumptions:

- the spacecraft in the constellation are in orbits that provide coverage of every point along a given latitude band (assuming said latitude band is visible from the selected orbit) without excessive overlap between passes: e.g. a controlled repeating ground-track orbit with a repeat period allowing at least x1 coverage of the viewable region per cycle;
- the spacecraft orbits have an inclination $i > 0$ and at least one region of interest lies at a latitude δ such that $|\delta| < i$;
- the field of view of the spacecraft is small relative to the Earth's surface and hence the Earth's surface can be treated as flat within this local region; and
- all spacecraft being considered are in circular orbits.

It should additionally be noted that for the purposes of this work, only the instantaneous filed-of-view of the spacecraft is considered. However, the method could be readily adapted to consider the field-of-regard of a slewable spacecraft if desired.

B. Coverage calculation

To estimate the number of spacecraft required to meet a defined coverage need, the circumference of the largest band of the Earth to be covered is used. For a constellation requiring global coverage, this will be the equator; for a constellation requiring regional coverage, this will be the latitude band of the region closest to the equator that is required to be covered. The number of orbit revolutions required for a single spacecraft to provide coverage of this widest band can then be calculated as

$$N_{rev} = \frac{c_\delta}{\alpha W_\delta} \tag{1}$$

where $\alpha = 2$ in the case that a single revolution will provide two usable passes of the latitude of interest (e.g. in the case of a radar instrument that can operate in all lighting conditions), and $\alpha = 1$ in the case that only one pass per revolution is usable (e.g. a visible light imager in a midnight-midday sun-synchronous orbit). Here, c_δ is the circumference of the latitude band of interest and W_δ is the width of this latitude band δ covered by a single pass of the spacecraft, which

depends on the direction of motion of the spacecraft relative to the line of latitude at nadir [16]. This can be calculated for spacecraft in circular orbits as

$$W_\delta = s\frac{1}{\sin\beta} = sF_\beta \tag{2}$$

where s is the spacecraft instrument swath width and $\beta = \tan^{-1}\left(\frac{\sqrt{\sin^2 i - \sin^2\delta}}{\cos i - \omega\cos^2\delta}\right)$ for a spacecraft in an orbit with inclination i, and where ω is the rotational rate of the Earth. F_β is defined in this work as the *swath scaling factor*, where $F_\beta \geq 1$ and defines the increase in effective swath width at a given latitude due to the ground track geometry.

It should be noted that as the latitude of interest δ approaches the orbit inclination i, the width covered W_δ will tend to infinite. As such, equation (1) is not valid at latitudes very close to i, however, as the latitude with the largest circumference band will be that closest to the equator in a given region of interest, it is unlikely that $\delta \approx i$. Assuming that coverage of the widest latitude band of interest will ensure coverage of all regions of interest, the time required to obtain full coverage of a region of interest can be estimated as

$$t = T\frac{N_{rev}}{N_{sats}} \tag{3}$$

where T is the satellite orbit period and N_{sats} is the number of spacecraft being used for observation.

C. Cloud circumference factor

In order to account for the impact of cloud cover, the concept of a *cloud circumference factor* $F_{\delta c}$ is introduced. This is a scaling factor that when multiplied by the circumference of the equator will provide a *psuedo-circumference* for a given latitude that can be used in place of c_δ in equation (1) to calculate the expected number of revolutions required to provide coverage of the selected latitude band, accounting for the impact of cloud cover probability. $F_{\delta c}$ incorporates the circumference of a given latitude and an appropriate representation of cloud cover probability, and is normalised against the circumference of Earth at the equator to allow direct comparison between latitudes. The *cloud circumference factor* $F_{\delta c}$ is calculated as

$$F_{\delta c} = \frac{c_\delta}{c_{eq}}\frac{\ln(1 - p_{obs})}{\ln(f_{\delta c})} \tag{4}$$

where $f_{\delta c}$ is the maximum value of mean cloud cover probability for all longitude points of interest along a given latitude band δ. This could be selected as the maximum value for the full latitude band, or restricted to the maximum value for only regions of interest - such as only land regions, or distinct countries or areas. In this way, the calculation can be tailored to the specific mission goals by considering cloud probability only over regions of interest. In equation (4), c_{eq} is the circumference of the Earth's equator, and p_{obs} is the desired probability of obtaining a cloud-free image

$(0 < p_{obs} < 1)$ [17]. For cases where the latitude of interest is the equator, $c_\delta = c_{eq}$ and hence $\frac{c_\delta}{c_{eq}} = 1$. In all cases, $F_{\delta c} \geq 1$.

A *pseudo-circumference*, $c_{\delta c}$, can subsequently be calculated for a given latitude to describe the imaginary circumference that would need to be covered to provide a desired probability of cloud free coverage of a given latitude. This is calculated as $c_{\delta c} = F_{\delta c} c_{eq}$. The time required to obtain full coverage of a region of interest considering the impact of cloud cover probability can hence be estimated as

$$t = max\left\{\frac{F_{\delta c}}{F_\beta} : \delta_{min} \leq \delta \leq \delta_{max}\right\} \frac{c_{eq} T}{s N_{sats}} \tag{5}$$

where $max\left\{\frac{F_{\delta c}}{F_\beta} : \delta_{min} \leq \delta \leq \delta_{max}\right\}$ is maximum value of the ratio of cloud circumference factor to swath scaling factor across all latitudes of interest.

D. Cloud cover data

Figure 1 shows the 2007 day-time data from the Cloud-Aerosol Lidar and Infrared Pathfinder Satellite Observation (CALIPSO) Cloud-Aerosol LIdar with Orthogonal Polarization (CALIOP) instrument*. This provides the mean cloud cover fraction for latitudes -80.55 deg to +76.57 deg in steps of 2 deg in latitude and longitude. This data is used in this paper for calculations using the presented analytical method, with the assumption that it provides a binary probability of cloud-free versus cloudy data (i.e. a 50% mean annual cloud cover fraction corresponds to a 50% probability of any acquired image being cloud-free). Alternative cloud cover data could be used without impacting the outlined method.

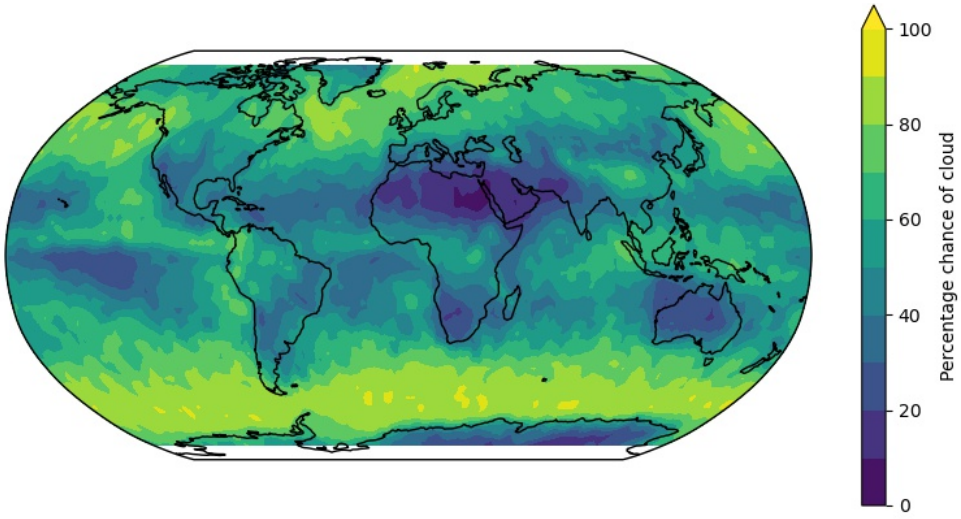

Fig. 1 Mean cloud cover probability at daytime in 2 deg grid of latitude and longitude from the Cloud-Aerosol Lidar and Infrared Pathfinder Satellite Observation (CALIPSO) Cloud-Aerosol LIdar with Orthogonal Polarization (CALIOP) instrument*.

*https://www-calipso.larc.nasa.gov

III. Results

A. Cloud circumference factor

Figure 2 shows the maximum mean cloud cover probability of each latitude from -80 deg to 76 deg (left) and the corresponding *cloud circumference factor* $F_{\delta c}$ (right) for an 80% probability of obtaining a cloud free image. If coverage of only certain regions is desired, the cloud cover data can be filtered to reflect this by considering, for example, only latitude bands of interest, or only geographical areas of interest (e.g. individual countries). These assessments by geographical region can provide valuable insights as seen in Figure 3 where only land is considered, and Figure 4 where only ocean is considered. From this it can be determined that the global results are primarily driven by the heavy cloud cover over ocean regions, with the cloud cover over land significantly less. It can be seen that when accounting for cloud in the case of global coverage, the -70 deg to -40 deg latitudes will be the most challenging to cover. If only land is of interest the spread is more evenly distributed across the latitudes with the equatorial regions the most challenging to cover. The null values seen in Figure 3 at approximately -55 to -60 degrees latitude are due to the fact that no land is identified within this latitude range at the 2 degree resolution used.

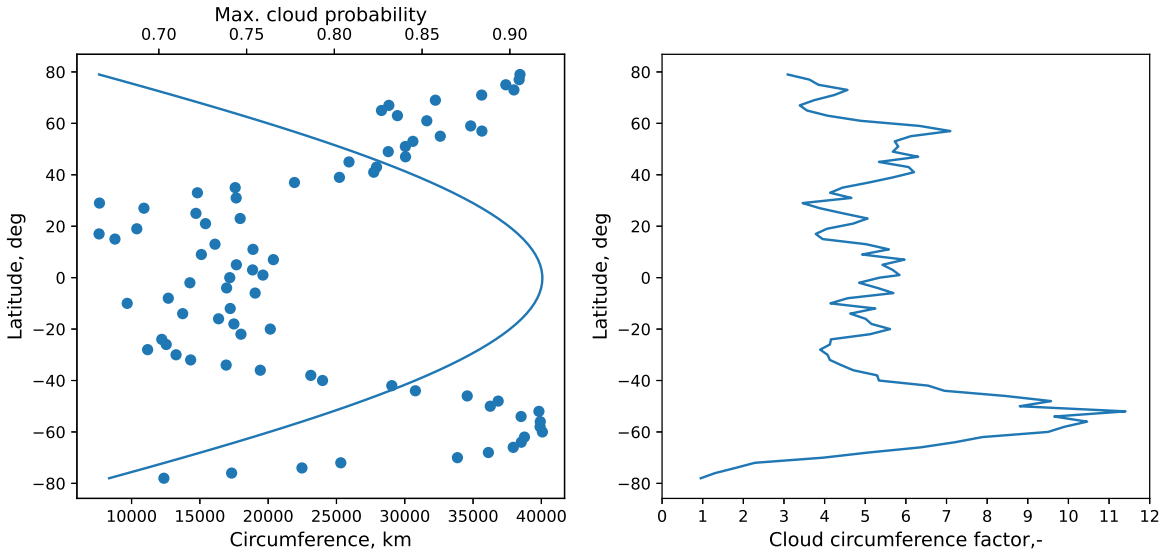

Fig. 2 (Left) Earth's circumference (line) and maximum mean cloud cover probability (scatter) as a function of latitude considering whole Earth. (Right) Cloud circumference factor as a function of latitude.

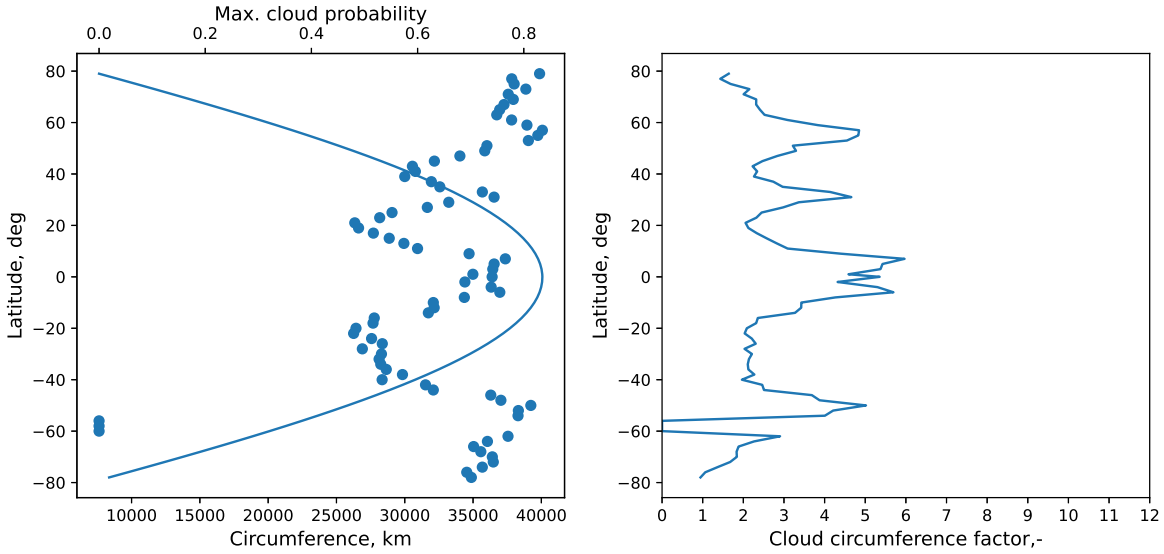

Fig. 3 (Left) Earth's circumference (line) and maximum mean cloud cover probability (scatter) as a function of latitude considering only land. (Right) Calculated cloud circumference factor for land as a function of latitude.

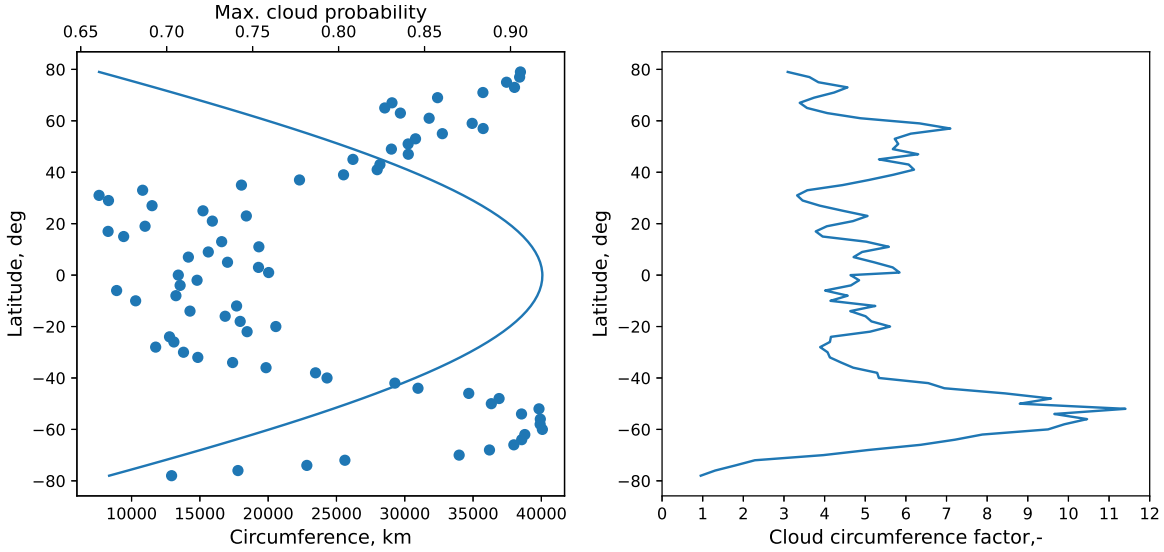

Fig. 4 (Left) Earth's circumference (line) and maximum mean cloud cover probability (scatter) as a function of latitude considering only ocean. (Right) Calculated cloud circumference factor for ocean as a function of latitude.

B. Comparison with simulated and historical data

To investigate the accuracy of the proposed method, a number of locations distributed in latitude and longitude are selected for investigation. The details of these are given in Table 1. The Sentinel-2 constellation is selected for this analysis and three different methods of cloud cover assessment are investigated:

1) Proposed analytical method;
2) Coverage analysis simulation using recorded daily-average cloud fraction;
3) Assessment of historical data using cloud cover percentages.

Table 1 Locations selected for cloud cover analysis.

Region	Latitude	Longitude
Solway Firth, UK	55°	-3.5°
Madrid, Spain	40°	-3.5°
Vilnius, Lithiuania	55°	25°
Bobo-Diolasso, Burkina Faso	11°	-4.3°

1. Proposed analytical method

The results in Table 2 show the total number of images of each region predicted to be collected in a year, as well as the mean time calculated as required to provide a 60%, 70%, 80% and 90% probability of obtaining a cloud-free image. This is calculated using the maximum cloud cover value for only the relevant country being considered, selected according to the geometric bounds of the country as defined by the ESRI World Countries - Generalized data set[†].

From the results in Table 2 it can be seen that the Solway Firth and Vilnius have similar results. This implies that latitude is the dominant factor determining the time needed to have a given probability of obtaining a cloud free image; this is as would be expected given that latitude bands tend to have similar cloud cover patterns. Madrid has a significantly higher likelihood of obtaining cloud free images than the other three regions. This is because it has a significantly lower cloud cover fraction (according to the selected data set) than the Solway Firth or Vilnius, and this more than makes up for the fewer number of passes by the spacecraft over Madrid as a result of its lower latitude. Although Madrid has a similar cloud fraction value as Bobo-Diolasso (approximately 40%), the lower latitude and hence fewer passes over Bobo-Diolasso results in a longer time needed to obtain the desired probability of a cloud free image.

Table 2 Results of analytical method indicating number of total images expected per year and mean time required to for given probability (% chance) of obtaining a cloud free image.

Region	Mean number of images per year	60%	70%	80%	90%
Solway Firth, UK	137	7 days	9 days	12 days	17 days
Madrid, Spain	99	4 days	5 days	6 days	9 days
Vilnius, Lithiuania	137	7 days	9 days	12 days	17 days
Bobo-Diolasso, Burkina Faso	78	6 days	7 days	10 days	14 days

2. Coverage analysis simulation

A numerically propagated simulator is used to provide a higher fidelity result than expected from the proposed analytical method. This simulator uses available observational data from space-track.org in the form of two-line elements (TLEs) [18]. The Skyfield python library [19] is used to propagate the satellites' orbits between two successive TLEs using an SGP4 propagation routine. This propagation method is then repeated between every TLE gathered over the year. Given both Sentinel 2A and 2B have a field of view of approximately 20.6°, a series of contacts is gathered at the

[†]https://hub.arcgis.com/datasets/esri::world-countries-generalized

desired target locations. The recorded contact dates are then compared with day-time mean cloud cover data from the Copernicus CLARA data set [20] and an estimate is made of the number of potential images the Sentinel-2 constellation could have captured of the target locations that contain cloud cover below a desired threshold. For some days, day-time mean cloud cover data is not available in the CLARA data set. For these days, the 24-hour mean cloud coverage value is used instead. The years 2018 - 2021 are considered to give reasonable averaged results, and only daytime passes are counted as usable within this simulation. The results of this analysis is given in Table 3.

Table 3 Results of coverage simulation indicating mean number of images per year (2018 - 2021 inclusive) expected to have a cloud cover fraction of <X%.

Region	Mean number of images per year	<10%	<20%	<30%	<40%
Solway Firth, UK	151	7%	12%	16%	19%
Madrid, Spain	73	23%	34%	42%	49%
Vilnius, Lithiuania	150	14%	18%	23%	26%
Bobo-Diolasso, Burkina Faso	73	38%	42%	47%	51%

3. Historical data assessment

In this approach, the historical imagery collected by the Sentinel-2 spacecraft constellation over the period of 2018 - 2022 is analysed. To avoid duplicated images, a combination of geolocation points and tile names corresponding to the geolocations have been selected: Solway Firth = 30UVF, Madrid = 30TVK, Vilnius = 35ULA, and Bobo-Diolasso = 30PUT. The naming of the tiles is according to THALES [21]. The tiles extend over 110 km $\times$ 110 km and the Sentinel-2 database can be queried by the names of each tile as well as the cloud cover percentage of the product image during acquisition time. Using this approach, the images collected over each of the regions within this time period are categorised according to the level of cloud cover seen in the image as shown in Table 4 for up to 40% cloud cover.

4. Comparison of methods

Comparing the mean number of total images collected per year across the methods shows a general consistency.The difference between the analytical method (Table 2) and the other methods in the case of Madrid can be explained by the averaging approach taken in the analytical method, which will not account for the fact that a given location may fall within, or outside, an area of repeated passes due to the repeating ground track.

Table 4 Percentage of images collected by the Sentinel-2 constellation with <X% cloud (2018 - 2022 inclusive).

Region	Mean number of images per year	<10%	<20%	<30%	<40%
Solway Firth, UK	130	12%	21%	27%	34%
Madrid, Spain	73	43%	50%	55%	60%
Vilnius, Lithiuania	140	15%	20%	25%	30%
Bobo-Diolasso, Burkina Faso	72	42%	48%	53%	60%

Table 5 Mean days between predicted or actual Sentinel-2 collections with <10% cloud, compared with calculated intervals needed to have 90% chance of obtaining cloud-free image.

Region	Analytical method	Coverage simulation	Historical data
Solway Firth, UK	17 days	36 days	23 days
Madrid, Spain	9 days	21 days	12 days
Vilnius, Lithiuania	17 days	17 days	17 days
Bobo-Diolasso, Burkina Faso	14 days	13 days	12 days

Table 6 Mean days between predicted or actual Sentinel-2 collections with <20% cloud, compared with calculated intervals needed to have 80% chance of obtaining cloud-free image.

Region	Analytical method	Coverage simulation	Historical data
Solway Firth, UK	12 days	20 days	13 days
Madrid, Spain	6 days	15 days	10 days
Vilnius, Lithiuania	12 days	13 days	13 days
Bobo-Diolasso, Burkina Faso	10 days	12 days	11 days

There is no agreed upon definition of a “cloud-free" image. Depending on the user needs, it is possible that even a heavily clouded image could be usable if the region of interest is not obscured. For the purposes of this work, cloud cover percentages of up to 40% are considered and compared. Noting that the cloud coverage criteria being used in the various methods differ, it is decided for the purposes of this initial investigation to compare the time between obtaining images with <X% cloud cover (as defined by the simulation and historical analysis approaches) with the time needed to have a 100-X% probability of obtaining a cloud free image (as calculated using the proposed analytical method). It should be noted that these values are not equivalent, and as such the comparisons provide only a first indication of the potential applicability of the proposed method. Tables 5, 6, 7, and 8 show the predicted, or actual, mean time between images collected with < 10%, < 20%, < 30% and < 40% cloud cover, respectively, using the simulation method and the historical data analysis, compared with the expected mean time required to provide a corresponding 90%, 80%, 70% and 60% chance of obtaining a cloud-free image, respectively, as calculated using the proposed analytical method and considering the maximum cloud cover value for only the relevant country being considered.

Table 7 Mean days between predicted or actual Sentinel-2 collections with <30% cloud, compared with calculated intervals needed to have 70% chance of obtaining cloud-free image.

Region	Analytical method	Coverage simulation	Historical data
Solway Firth, UK	9 days	16 days	10 days
Madrid, Spain	5 days	12 days	9 days
Vilnius, Lithiuania	9 days	11 days	10 days
Bobo-Diolasso, Burkina Faso	7 days	11 days	10 days

Table 8 Mean days between predicted or actual Sentinel-2 collections with <40% cloud, compared with calculated intervals needed to have 60% chance of obtaining cloud-free image.

Region	Analytical method	Coverage simulation	Historical data
Solway Firth, UK	7 days	12 days	8 days
Madrid, Spain	4 days	10 days	8 days
Vilnius, Lithiuania	7 days	10 days	9 days
Bobo-Diolasso, Burkina Faso	6 days	10 days	8 days

IV. Discussion

The results presented in section III show reasonable agreement between the proposed analytical method, the simulation, and the analysis of the historical data. This implies there is merit in the proposed approach as a means of predicting expected performance of a constellation when considering cloud cover. The results, however, do differ across all three methods, particularly for the Solway Firth and Madrid regions. Surprisingly, the simulation shows a larger difference than the proposed analytical method in predicted number of days between cloud-free acquisitions when compared with the historical data for both the Solway Firth and Madrid. This implies that appropriate selection of cloud data is important to provide reliable results. Noting that the simulation makes use of daily-averaged data, it is theorised that these differences may occur due to a high variation in cloud cover throughout the day in coastal regions (such as Western Europe) which results in a poor estimation of cloud cover when average across the day. In fact, given the consistent overpass time of Sentinel-2 over each location, and knowing that one of the criteria for the selection the Sentinel-2 local time of ascending node was to provide overpasses with low cloud cover[‡], using cloud values measured at the precise overpass time each day and averaging these across the year may have been more appropriate and given greater agreement with the historical data.

The correlation between methods is based on the observation that true and simulated acquisition times between images with <X% cloud cover agree well with the calculated time needed to get a 100-X% chance of a cloud free image. This is a significant assumption and should be investigated for wider data sets and regions to assess its validity. If cloud-free imagery is taken to be that with < 10% cloud cover, then it can alternatively be said that for the cases considered, the proposed analytical method provides good predictions when it is set to predict the time needed to have a 90% chance of obtaining a cloud-free image. Assessing the sensitivity of the results to the selected probability value could provide insights into the nature of this correlation and inform selection of suitable values for future analyses.

It is of note that the proposed method does not consider the acquisition schedule of the satellite, or satellite constellation, nor does it account for repeated overlaps in coverage as seen in the Sentinel-2 repeating ground track. This could theoretically be accounted for by providing an adjustment factor to the calculated values as a function of latitude and/or longitude, if desired.

[‡]https://sentinels.copernicus.eu/web/sentinel/missions/sentinel-2/satellite-description/orbit

All data and methods within this paper require averaging over long periods of time as cloud cover can vary significantly, even between years. As such, the results should be interpreted as expected long terms averages. Monthly or even annual data can be expected to differ significantly from these averages. Furthermore, it should be noted that a mean number of days between acquisitions should not be expected to translate to an even distribution of cloud-free images. In reality, cloud-free acquisitions are likely to be more frequent during certain seasons, with extended gaps between clear images during poor weather periods. Using monthly cloud cover values averaged across multiple years within the proposed method could allow these seasonal variations to be considered.

V. Conclusion

The impact of cloud cover on satellite coverage can be quickly assessed using analytical approximations of coverage and cloud cover probabilities derived from historical data. By considering the maximum cloud cover of a region of interest, a pseudo-circumference value can be created as a function of latitude to assess expected mean time between cloud-free observations and inform mission designs. The approach can be restricted to consider only regions of interest, such as individual countries, enabling designs to be tailored to these regions, while use of seasonal or time-specific cloud models can provide insights into specific operational concepts. It is evident from the results shown using this method that cloud-free time to full coverage does not necessarily align with cloud-inconsiderate time to coverage. Higher-latitude regions can no longer be assumed to be fully covered faster than their lower-latitude counterparts, with cloud cover exhibiting significant, and non-trivial, impacts on revisit times. Using the Sentinel-2 constellation as an example, the results of the proposed analytical method show reasonable agreement with simulated and actual historical data when cloud cover percentage is aligned with the desired probability of obtaining a cloud free image; that is, the mean number of days between collected images with X% cloud cover shows reasonable agreement with the predicted number of days needed to have a 100 - X% chance of obtaining a cloud-free image. Further development of the work to account for acquisition schedules and orbit cross-over points would increase utility, while comparison across wider geographical areas and considering alternative cloud models would provide further valuable insight and indicate the potential value of the approach for mission analysis and planning.

Acknowledgments

This material is based partly upon work supported by the Air Force Office of Scientific Research under award number FA8655-22-1-7010. The authors would also like to thank Steven Hancock and Ian Davenport of the University of Edinburgh for providing some of the cloud data used in this paper.

References

[1] Walker, J. G., "Circular orbit patterns providing continuous whole earth coverage," Tech. rep., Royal Aircraft Establishment Farnborough (United Kingdom), 1970.

[2] Walker, J. G., "Continuous whole-earth coverage by circular-orbit satellite patterns," Tech. rep., Royal Aircraft Establishment Farnborough (United Kingdom), 1977.

[3] Ely, T., Crossley, W., and Williams, E., "Satellite constellation design for zonal coverage using genetic algorithms," *The journal of the Astronautical Sciences*, Vol. 47, 1999, pp. 207–228. https://doi.org/10.1007/BF03546200.

[4] Rider, L., "Analytic design of satellite constellations for zonal earth coverage using inclined circular orbits," *Journal of the Astronautical Sciences*, Vol. 34, 1986, pp. 31–64.

[5] Lüders, R., and Ginsberg, L., "Continuous zonal coverage-a generalized analysis," *Mechanics and Control of Flight Conference*, 1974, p. 842. https://doi.org/10.2514/6.1974-842.

[6] Abdelkhalik, O., and Gad, A., "Optimization of space orbits design for Earth orbiting missions," *Acta Astronautica*, Vol. 68, No. 7-8, 2011, pp. 1307–1317. https://doi.org/10.1016/j.actaastro.2010.09.029.

[7] Beste, D. C., "Design of satellite constellations for optimal continuous coverage," *IEEE Transactions on Aerospace and Electronic Systems*, Vol. AES-14, No. 3, 1978, pp. 466–473. https://doi.org/10.1109/TAES.1978.308608.

[8] Ulybyshev, Y., "Geometric analysis and design method for discontinuous coverage satellite constellations," *Journal of Guidance, Control, and Dynamics*, Vol. 37, No. 2, 2014, pp. 549–557. https://doi.org/10.2514/1.60756.

[9] Ulybyshev, Y., "Satellite constellation design for complex coverage," *Journal of Spacecraft and Rockets*, Vol. 45, No. 4, 2008, pp. 843–849. https://doi.org/10.2514/1.35369.

[10] Ulybyshev, Y., "General analysis method for discontinuous coverage satellite constellations," *Journal of Guidance, Control, and Dynamics*, Vol. 38, No. 12, 2015, pp. 2475–2483. https://doi.org/10.2514/1.G001254.

[11] McGrath, C. N., Cowley, D. C., Hood, S., Clarke, S., and Macdonald, M., "An assessment of high temporal frequency satellite data for historic environment applications. A case study from Scotland," *Archaeological Prospection*, 2022. https://doi.org/10.1002/arp.1890.

[12] McGrath, C. N., Scott, C., Cowley, D., and Macdonald, M., "Towards a satellite system for archaeology? Simulation of an optical satellite mission with ideal spatial and temporal resolution, illustrated by a case study in Scotland," *Remote Sensing*, Vol. 12, No. 24, 2020, p. 4100. https://doi.org/10.3390/rs12244100.

[13] Ju, J., and Roy, D. P., "The availability of cloud-free Landsat ETM+ data over the conterminous United States and globally," *Remote Sensing of Environment*, Vol. 112, No. 3, 2008, pp. 1196–1211. https://doi.org/10.1016/j.rse.2007.08.011.

[14] Sales, V. G., Strobl, E., and Elliott, R. J., "Cloud cover and its impact on Brazil's deforestation satellite monitoring program: Evidence from the cerrado biome of the Brazilian Legal Amazon," *Applied Geography*, Vol. 140, 2022, p. 102651. https://doi.org/10.1016/j.apgeog.2022.102651.

[15] Zuo, M., Dai, G., Peng, L., and Wang, M., "An envelope curve-based theory for the satellite coverage problems," *Aerospace Science and Technology*, Vol. 100, 2020, p. 105750.

[16] Washburn, A. R., "Earth Coverage by Satellites in Circular Orbit," *Department of operations Research Naval Postgraduate School*, 2004.

[17] Hancock, S., McGrath, C., Lowe, C., Davenport, I., and Woodhouse, I., "Requirements for a global lidar system: spaceborne lidar with wall-to-wall coverage," *Royal Society open science*, Vol. 8, No. 12, 2021, p. 211166. https://doi.org/10.1098/rsos.211166.

[18] Space-Track, "space-track.org," , 2023. URL https://www.space-track.org/.

[19] Rhodes, B., "Skyfield: High precision research-grade positions for planets and Earth satellites generator," Astrophysics Source Code Library, record ascl:1907.024, Jul. 2019.

[20] Karlsson, K., Anttila, K., Trentmann, J., Stengel, M., Meirink, J., Devasthale, A., Hanschmann, T., Kothe, S., Jääskeläinen, E., Sedlar, J., Benas, N., van Zadelhoff, G., Schlundt, C., Stein, D., Finkensieper, S., Håkansson, N., Hollmann, R., Fuchs, P., and Werscheck, M., "CLARA-A2: CM SAF cLoud, Albedo and surface RAdiation dataset from AVHRR data - Edition 2," , 2017. https://doi.org/10.5676/EUM_SAF_CM/CLARA_AVHRR/V002, URL https://cds.climate.copernicus.eu/cdsapp#!/dataset/satellite-cloud-properties?tab=overview.

[21] THALES, "Sentinel-2 Products Specification Document," Tech. rep., European Space Agency, 2021.